J. Geophys. 42, 15–25, 1976

Journal of Geophysics

Auroral Lyman-Alpha Emission

V. Dose, U. Schmocker and G. Sele

Physikalisches Institut der Universität Würzburg,
D-8700 Würzburg, Röntgenring 8, Federal Republic of Germany

Abstract. We have recently published new measurements on the electronic stopping power of molecular oxygen and nitrogen for protons with energies between 1 KeV and 30 KeV. These results together with known cross sections for excitation of Lyman-Alpha radiation in collisions of H^+, H^0 and H^- with the atmospheric gases are used to predict auroral Lyman-Alpha emissions. We obtain heights for maximum Lyman-Alpha production which are considerably lower than those obtained using the earlier range data of Cook *et al.* [1953]. Assuming the velocity dependence of the Lyman-Alpha emission cross sections to be similar to the up to now unknown H-Beta cross sections, a comparison of rocket flight data from the experiments of Wax and Bernstein and Miller and Shepherd with the present calculations gives encouraging agreement.

Key words: Lyman-Alpha radiation – Height profiles – Stopping power – Aurora.

I. Introduction

Vegard (1939) was the first to observe hydrogen lines in the auroral spectrum. The discovery of a considerable Doppler-shift of the hydrogen emissions led to the conclusion, that these lines were due to fast protons entering the earths atmosphere during auroras. Many observations have been made since and a big amount of theoretical work has been done to interpret auroral hydrogen emissions. Comprehensive reviews are given by Chamberlain (1961), Eather (1967), and Omholt (1971).

Reliable calculations, however, are only possible if the necessary laboratory data on the emission of hydrogen lines in collisions of protons, fast hydrogen atoms and negative hydrogen ions with atmospheric gases are available. In addition to emission cross sections, data on charge equilibrated hydrogen beams and on the stopping of hydrogen projectiles in atmospheric gases are needed. A review of the presently available laboratory data has been recently published by Mc Neal and Birely (1973). We have carried out a few additional measurements on Lyman-Alpha emission in collisions of H^- with nitrogen and oxygen. A complete set of data on production of Lyman-Alpha radiation in collisions of hydrogen projectiles with atmospheric gases is therefore now available. Since data on charge equilibrated hydrogen beams are also well known (Allison and Garcia-Munoz, 1962; Tawara and Russek, 1973) it is possible using a proper atmospheric model and appropriate data on the stopping of protons to apply these results to auroral Lyman-Alpha emission.

Similar calculations with a less complete set of laboratory data have been carried out previously employing the range measurements of Cook *et al.* (1953). Recent measurements on the stopping power of nitrogen and oxygen for protons with energies between 1 KeV and 30 KeV carried out in our laboratory (Dose and Sele, 1975), however, showed that estimates of range for low energy protons obtained from an extrapolation of Cook's data bear a considerable error.

In this paper we report calculations on auroral Lyman-Alpha emission using the new stopping cross sections. The CIRA 72 standard atmosphere is adopted as the atmospheric model. Assuming the velocity dependence of the Lyman-Alpha emission cross sections to be similar to corresponding and up to now unknown H-Beta emission cross sections, a comparison of our calculations with rocket flight observations on H-Beta emission from two different experiments (Wax and Bernstein, 1970; Miller and Shepherd, 1969) yields encouraging agreement.

II. Excitation of Lyman-Alpha Emission

The excitation of Lyman-Alpha emission may be calculated by the equations of statistical equilibrium (Chamberlain, 1954). Take the number density of atmospheric atoms (counting a diatomic molecule as two atoms) to be N_a. Let F_i^∞ be the fraction of hydrogen projectiles in charge state i and Q_{i-2p} the cross section for excitation of the hydrogen in charge state i to the $2p$ state. The volume emission rate of Lyman-Alpha radiation F_{21} per unit incident flux neglecting cascading effects is the given by

$$F_{21} = N_a \{F_1^\infty Q_{1-2p} + F_0^\infty Q_{0-2p} + F_{\bar{1}}^\infty Q_{\bar{1}-2p}\}. \tag{1}$$

The equilibrium fractions are readily obtained in terms of charge changing cross sections as given by Tawara and Russek (1973). Cross sections for excitation of Lyman-Alpha radiation in collisions of H and H^+ with molecular nitrogen and oxygen are available from the review of Mc Neal and Birely (1973) as well as from unpublished work in our own laboratory. Cross sections $Q_{\bar{1}-2p}$ were recently determined in our laboratory and will be published elsewhere. All emission cross sections were approximated for the present purpose by analytical expressions of the form

$$Q = \sum_{n=1}^{N} \frac{a_n v^n}{(b+v)^{n+1}} \tag{2}$$

where v is the projectile velocity in atomic units. The coefficients a_n are given in Table 1.

Table 1. Coefficients for the analytical approximation to Lyman-Alpha emission cross sections as in Eq. (2). The velocity is taken in atomic units. The cross section is in units of 10^{-17} cm^2 per molecule

	N_2			O_2		
	Q_{1-2p}	Q_{0-2p}	$Q_{\bar{1}-2p}$	Q_{1-2p}	Q_{0-2p}	$Q_{\bar{1}-2p}$
b	0.3130	0.4174	1.055	0.3130	0.3130	1.45
a_1	0.662794	4.09415	247.625	9.36979	−0.67063	397
a_2	−21.4369	19.0505	−1,217	−3.94790	20.0677	−2,522
a_3	106.194	−26.4665	2,570	32.6035	−16.8208	6,552
a_4	−93.8669	44.3644	−1,964	−93.0553	−	−5,896
a_5	−	−50.2562	−	−37.7109	−	−
a_6	−	−	−	55.0455	−	−
a_7	−	−	−	395.936	−	−
a_8	−	−	−	−393.541	−	−

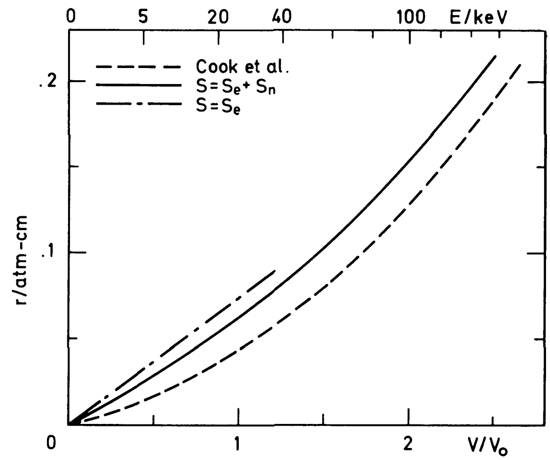

Fig. 1. Residual range of protons in a standard atmosphere composed of 80% N_2 and 20% O_2. The upper-dash-dotted curve was calculated using the electronic stopping power S_e measured in our laboratory. The solid curve is the atomic stopping power calculated from S_e as before with theoretically calculated contributions S_n from elastic scattering by the nuclei. The lower dashed curve is from the experiment of Cook *et al.* (1953)

The volume emission rate F_{21} is a function of the projectile energy. We calculated F_{21} for a constant density atmosphere. In this case it is more convenient, to take the residual range of the projectiles as the independent variable. The residual range is, in turn, a unique function of the atomic stopping power of the respective gases. The only direct range measurement available is that of Cook *et al.* (1953) for energies $E \geqq 7$ KeV in the case of nitrogen and $E \geqq 13$ KeV in the case of oxygen. Several measurements have been carried out on the electronic stopping power S_e of oxygen and nitrogen (Jesse and Sadauskis, 1950; Reynolds *et al.*, 1953; Phillips, 1953; Ormrod, 1968; Dose and Sele, 1975) mostly at even higher energies. For the present purpose we take the most recent data from the work of Dose and Sele (1975) for energies between 1 KeV and 30 KeV and the results of Reynolds *et al.* (1953) for $E \geqq 30$ KeV. To obtain the atomic stopping power, the nuclear stopping power S_n, which is a small correction at all energies, is calculated from theoretical work of Lindhard *et al.* (1963) and Schiott (1966). Fig. 1 shows the resulting residual range of protons in a constant density atmosphere composed of 80%

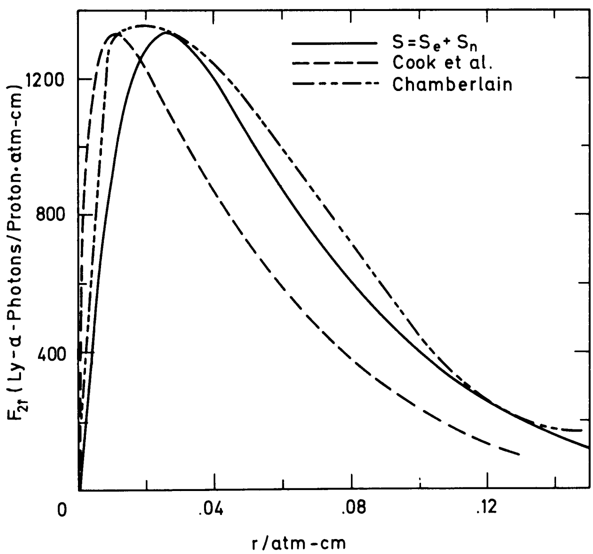

Fig. 2. The emission rate of Lyman-Alpha photons per unit volume per proton as a function of the proton residual range. The upper dash-dotted curve is Chamberlain's estimate (1961) reduced by a factor of four. The lower dashed curve was computed using Cook's range data (1953) while the solid curve is obtained with the range-energy relation of this work

nitrogen and 20% oxygen. The lower dashed curve gives the results of Cook *et al.* (1953) with extrapolation in the low energy region. The upper dashed line is obtained using the electronic stopping power S_e (Dose and Sele, 1975) only, while the solid curve is calculated adding the theoretically computed stopping power S_n to the experimental data on S_e from Dose and Sele (1975) and Reynolds *et al.* (1953). The solid curve is quite accurately given by

$$E = 27.4531\, r + 6{,}611.5\, r^2 - 15{,}863\, r^3 \tag{3}$$

with E in KeV and r in atm-cm. Cook's results are approximated by

$$\ln(E/30) = 1.286 \ln(r/0.05). \tag{4}$$

Fig. 2 shows the volume emission rate F_{21} as a function of the proton residual range r. The solid curve is the result of this work using cross sections as given by (2) and Table 1 together with the range energy relation (3). The lower dashed curve is obtained with the range-energy relation (4). The upper dash-dotted curve is an estimate by Chamberlain (1961) which was divided by a factor of four in order to fit into the present picture. F_{21} may be expressed accurately in analytical form by

$$F_{21}(r) = \sum_{n=1}^{4} \frac{a_n r^n}{(b+r)^{n+1}} \tag{5}$$

with coefficients as given in Table 2. The calculations displayed in Fig. 2 include contributions due to H^-. The relative importance of H^-, however, remains small everywhere as shown in Fig. 3. This is mainly due to the small fraction of H^- ions in a charge equilibrated hydrogen beam, although the cross sections for production of Lyman-Alpha radiation are larger by roughly a factor of three for H^- impact than those for proton or hydrogen atom impact.

Table 2. Coefficients for the analytical representation of the volume emission rate $F_{21}(r)$ of Lyman-Alpha radiation as a function of residual proton range r. With r in atm-cm F_{21} is given as the number of Lyman-Alpha photons produced per proton and atm-cm

Range-energy relation	(3)	(4)
b	0.0381	0.02
a_1	107.453	261.656
a_2	727.625	−807.032
a_3	−1,299.12	1,443.62
a_4	326.375	−963.375

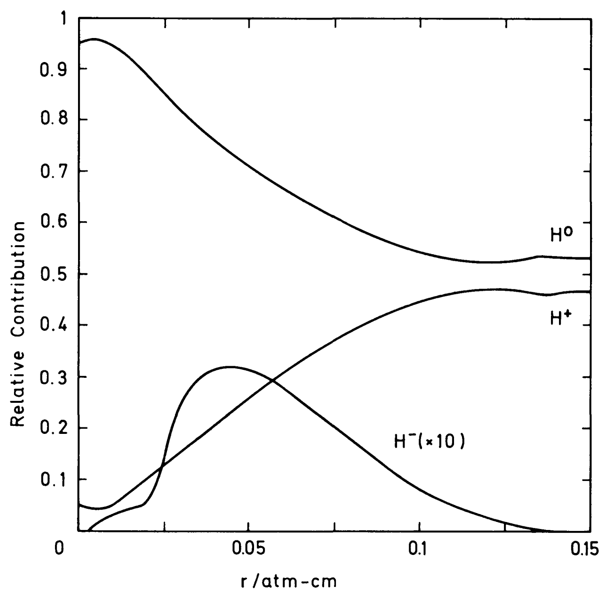

Fig. 3. Relative contribution of the different hydrogen charge states to the production of Lyman-Alpha radiation. The H^- contribution is always smaller than 3% due to the low fraction of H^- ions in a charge equilibrated hydrogen beam

The total number of Lyman-Alpha photons Z_{21} for a proton of given initial energy E_0 is the area under the curves in Fig. 2.

$$Z_{21} = \int_0^{r(E_0)} F_{21}(r')\,dr'. \tag{6}$$

Fig. 4 shows a plot of Z_{21} versus E_0. The solid curve is obtained using the range energy relation (3) while the dashed curve is obtained with (4). The difference is most pronounced for low initial energies $E \leqq 25$ KeV. The upper dash-dotted curve is an estimate used by Clark and Metzger (1969) to correlate auroral Lyman-Alpha emission observations with incident proton flux. Their result is based on an estimate by Eather (1967) of 360 photons per 300 KeV proton. This figure as well as Chamberlain's estimate (1961) of 460 photons per proton appears to be much too high.

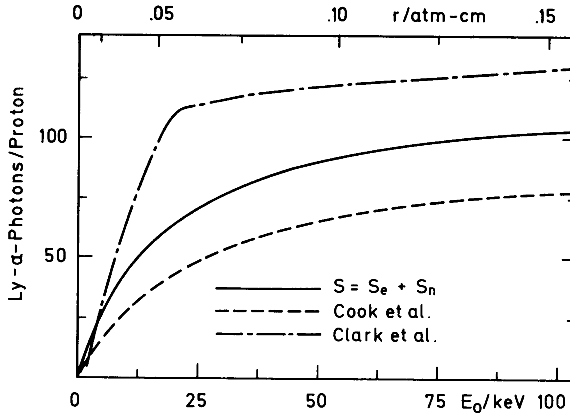

Fig. 4. The total number of Lyman-Alpha photons produced by a proton of given initial energy. The solid curve was computed employing the range-energy relation of this work. The lower dashed curve is obtained with Cook's data and the upper dash-dotted curve is an estimate by Clark and Metzger (1969)

III. Lyman-Alpha Emission in the CIRA 72 Standard Atmosphere

A. Normally Incident Monoenergetic Protons

The results of Section II may be converted to actual atmospheric emissions with the help of an atmospheric model. We have chosen the CIRA 72 standard atmosphere data. The equivalent atmospheric depth ξ in atm-cm is given in terms of actual height h as

$$\xi(h)=\frac{1}{2\,n_0}\int_h^{\infty}\{2\,n(N_2)+2\,n(O_2)+n(O)\}\,dh' \tag{7}$$

where n_0 is Loschmidt's number and n is the particle number density as given in CIRA 72. The inverse relation $h(\xi)$ may be conveniently expressed as

$$h=\sum_{k=0}^{3} a_k(\ln\xi-\ln\xi_0)^{2k} \tag{8}$$

with h in km and ξ in atm-cm. The constants are

$a_0=99.3828,\qquad a_2=\ \ 2.36435\cdot 10^{-2},$

$a_1=\ 0.726563,\qquad a_3=-9.22684\cdot 10^{-5},$

$\xi_0=\ 1.5683.$

With the help of (8) the volume emission rate F_{21} as a function of height is given by

$$F_{21}(h)=-F_{21}(\xi)\cdot\frac{d\xi}{dh}. \tag{9}$$

Fig. 5 shows examples for initial proton energies of 8 KeV and 20 KeV. Solid curves are obtained with the range-energy relation (3) and dashed curves with (4). The effect is drastic and it is suggestive that recent efforts to obtain agreement between observed and calculated H-Beta emissions (Wax and Bernstein, 1970; Miller and Shepherd, 1969) failed because the stopping power used was too high.

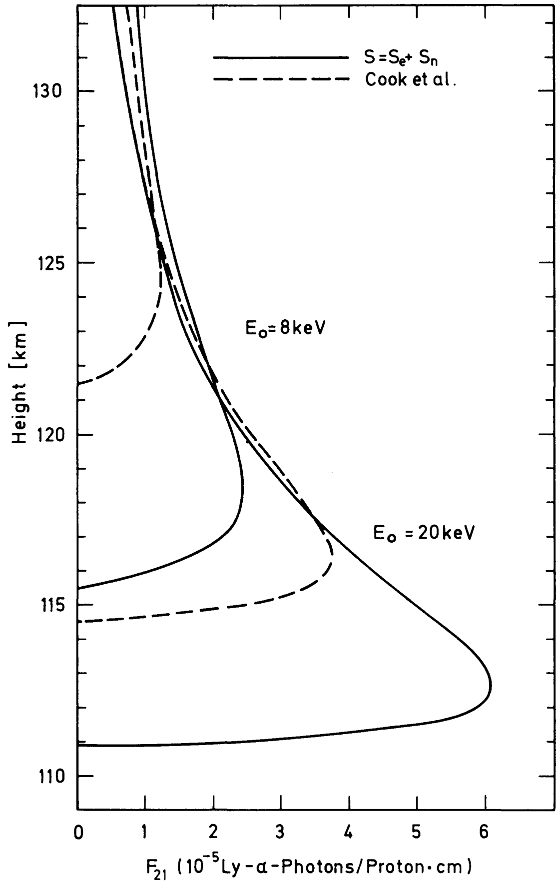

Fig. 5. Height profile of the volume emission rate for production of Lyman-Alpha radiation by normally incident monoenergetic protons of 8 KeV and 20 KeV initial energy in the atmosphere. The CIRA 72 standard atmosphere was used as the atmospheric model. Dashed curves were computed using Cook's range data while solid curves were obtained employing the range-energy relation of this work. A drastic change in the height of peak emission is observed

B. Emission Height Profiles for Given Energy and Pitch Angle Distributions

A convenient and sufficiently flexible pitch angle distribution has been proposed by Chamberlain (1954). If ϑ is the angle against a line normal to the atmosphere then

$$f(\vartheta)=\frac{N+2}{2\pi}\cos^N\vartheta. \tag{10}$$

Let $g(r_0)$ be the energy distribution of the incident protons with the energy E expressed by the initial range r_0. The number of Lyman-Alpha photons emitted per proton and atm-cm is then given as a function of equivalent depth by (Chamberlain, 1961; Eather, 1967)

$$F_{21}(\xi)=(N+2)\,\xi^{N+1}\int_{\xi}^{\infty} g(r_0)\,dr_0\int_0^{r_0-\xi}\frac{F_{21}(r)}{(r_0-r)^{N+2}}\,dr \tag{11}$$

where r is the residual range. Actual emission height profiles are again obtained using (9). With the analytic representation of F_{21} given in Section II the inner integration may be carried out analytically. The remaining integration over the

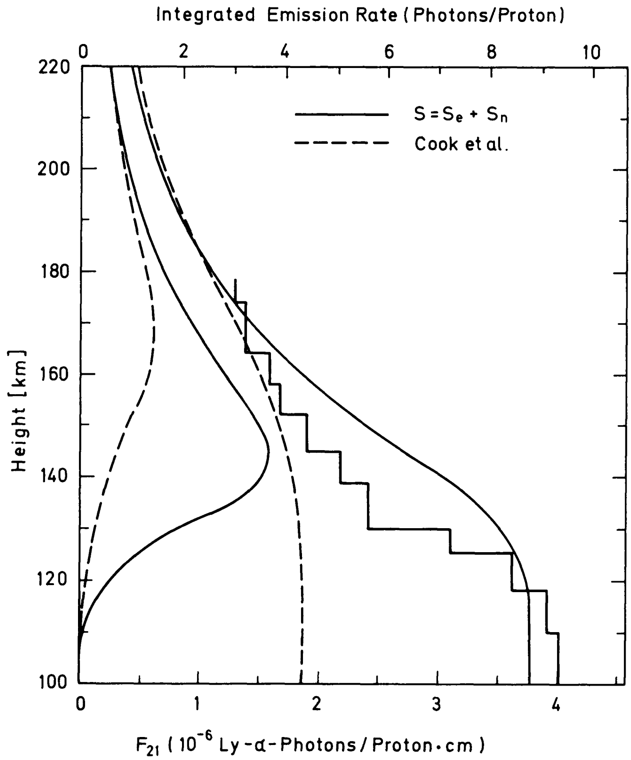

Fig. 6. Height profile and integrated emission rate of Lyman-Alpha radiation produced by protons with an isotropic pitch angle distribution and a power law $E^{-3.2}$ energy spectrum. Solid curves are computed using the range-energy relation of this work and dashed curves are obtained using Cook's range data. The staircase curve is a rocket flight observation of H-Beta radiation from the experiment of Wax and Bernstein (1970)

energy distribution must be done numerically. Of course, there is no unique choice for the energy distribution $g(r_0)$. In fact, strong variations are observed on different occasions (Mc Neal and Birely, 1973). Moreover, since no observations on height profiles for Lyman-Alpha emission have come to our attention, it would appear to be useless to proceed further. However, if we make the reasonable assumption, that cross sections for emission of H-Beta radiation exhibit a velocity dependence similar to Lyman-Alpha excitation cross sections, a comparison to recent rocket flight data is possible. Two rather different sets of observations are available. Wax and Bernstein (1970) measured the integrated emission rate of H-Beta radiation and the particle energy spectrum between 0.5 KeV and 22 KeV during an auroral break up above Fort Churchill. They found that the hydrogen differential energy spectrum fitted very well to a power law E^{-n} with $n=3.2$. We insert this energy distribution in (11), carry out the numerical integration assuming an isotropic pitch angle distribution and arrive at the result shown in Fig. 6.

Rocket observations are displayed by the staircase line. Calculations for both, the integrated emission rate along the line of sight and the volume emission rate as a function of height are shown. Dashed lines are obtained with the conventional range energy relation (4) while solid curves are obtained with the new relation (3). Evidently the latter results are much superior. In particular, the shift in peak emission height from 170 km to 145 km is most remarkable because Wax and

Fig. 7. Height profile and integrated emission rate of Lyman-Alpha radiation produced by protons with an isotropic pitch angle distribution and an energy spectrum corresponding to the auroral conditions in the rocket experiment of Miller and Shepherd (1969). Solid curves are computed using the range energy relation of this work while dashed curves are obtained with Cook's range data. Solid circles and squares are from H-Beta measurements in the rocket flight experiment of Miller and Shepherd (1969)

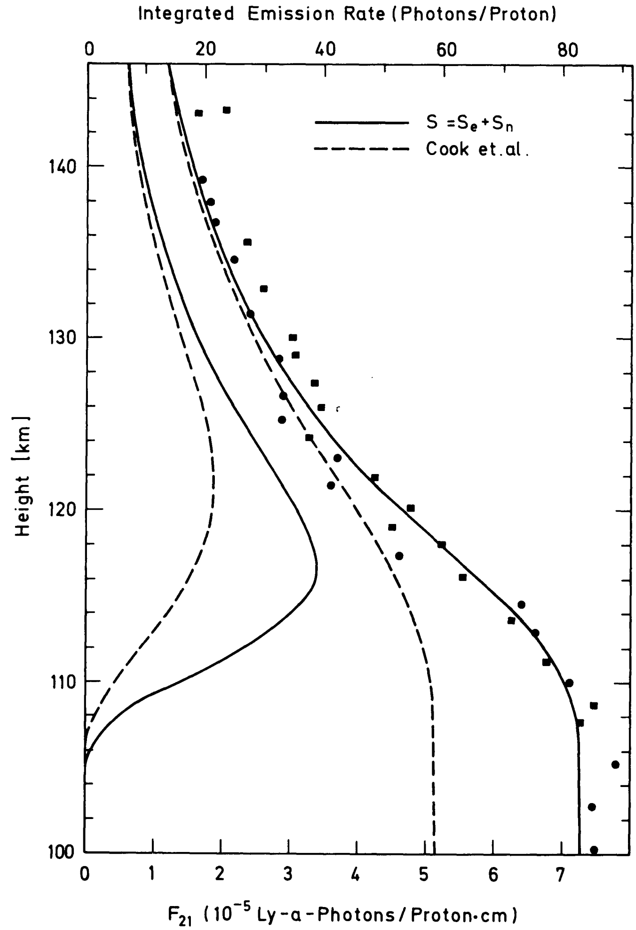

Bernstein (1970) being unable to get agreement between their observations and calculations, were even prepared to suggest a reduced atmospheric density above Fort Churchill.

The second set of observational data was evaluated from a rocket flight into a quiet evening hydrogen arc at Fort Churchill by Miller and Shepherd (1969). The particle energy spectrum was derived from proton energy measurements for $E \geqq 30$ KeV in combination with accepted H-Beta Doppler profile shapes. The derived energy spectrum was approximated by an *e*-folding energy of 12 KeV with a cut-off at 23 KeV plus "a certain amount" of low energy particles. We have represented the low energy particle component by the constant $\exp\{-23/12\}$ for $10\,\text{KeV} \leqq E \leqq 23$ KeV and zero for $E \leqq 10$ KeV. A guess of this kind is suggested by observations of Whalen *et al.* (1971) and Whalen and Mc Diarmid (1972). Using this energy distribution and an isotropic pitch angle distribution we arrive at the results shown in Fig. 7. Again both, integrated emission rate and height profile are shown. Dashed curves are obtained with range energy relation (4), while solid curves were calculated using (3). The agreement between the latter results and observations is surprisingly good. In particular, the height of the peak emission rate of 116 ± 2 km as quoted by Miller and Shepherd (1969) is excellently reproduced.

Considering the agreement between our calculations and the two strongly differing sets of observational data the underlying assumption concerning the velocity dependence of the H-Beta production cross sections seems to be well justified.

IV. Conclusions

The present calculations have shown that emission rate profiles and integrated emission rates depend quite sensitively on the range-energy relationship employed. Comparative calculations on Lyman-Alpha emission with a new range-energy relation constructed from recent laboratory measurements of the electronic stopping power S_e of atmospheric gases and theoretically calculated corrections for nuclear contributions S_n and with earlier data from the experiment of Cook *et al.* (1953) suggest that part of the difficulties in interpreting auroral hydrogen emissions can be overcome by using the correct stopping power. In fact, Lyman-Alpha emission cross sections together with our range energy relation reproduce surprisingly well two sets of rocket flight data of H-Beta emission which were taken under rather different auroral conditions. The agreement achieved seems to support the assumption that the velocity dependence of hydrogen emission cross sections is similar for different principal quantum numbers.

References

Allison, S. K., Garcia-Munoz, M.: Electron capture and loss at high energies. In: Atomic and molecular processes, D. R. Bates, ed.: pp. 722–780. New York-London: Academic Press 1962

Chamberlain, J. W.: The excitation of hydrogen in aurorae. Astrophys. J. **120**, 360–366, 1954

Chamberlain, J. W.: Physics of the aurora and airglow. New York: Academic Press 1961

Clark, M. A., Metzger, P. H.: Auroral Lyman-alpha observations. J. Geophys. Res. **74**, 6257–6265, 1969

Cook, C. J., Jones, E., Jorgensen, T.: Range-energy relations of 10- to 250-KeV protons and helium ions in various gases. Phys. Rev. **91**, 1417–1422, 1953

Dose, V., Sele, G.: Electronic stopping power of nitrogen and oxygen for low energy protons. Z. Physik A **272**, 237–243, 1975

Eather, R. H.: Auroral proton precipitation and hydrogen emissions. Rev. Geophys. **5**, 207–285, 1967

Jesse, W. P., Sadauskis, J.: The range-energy curves for alpha-particles and protons. Phys. Rev. **78**, 1–8, 1950

Lindhard, J., Scharff, M., Schiott, H. E.: Range concepts and heavy ion ranges (Notes on atomic collisions, II). Dan. Mat. Fys. Medd. **33**, No. 14, 1963

Mc Neal, R. J., Birely, J. H.: Laboratory studies of collisions of energetic H^+ and hydrogen with atmospheric constituents. Rev. Geophys. and Space Phys. **11**, 633–692, 1973

Miller, J. R., Shepherd, G. G.: Rocket measurements of H beta production in a hydrogen aurora. J. Geophys. Res. **74**, 4987–4997, 1969

Omholt, A.: The optical aurora. Berlin-Heidelberg-New York: Springer 1971

Ormrod, J. H.: Low-energy electronic stopping cross sections in nitrogen and argon. Can. J. Phys. **46**, 497–502, 1968

Phillips, J. A.: The energy loss of low energy protons in some gases. Phys. Rev. **90**, 532–537, 1953

Reynolds, H. K., Dunbar, D. N. F., Wenzel, W. A., Whaling, W.: The stopping cross section of gases for protons, 30–600 KeV. Phys. Rev. **92**, 742–748, 1953

Schiott, H. E.: Range-energy relations for low-energy ions. Dan. Mat. Fys. Medd. **35**, No. 9, 1966

Tawara, H., Russek, A.: Charge changing processes in hydrogen beams. Rev. Mod. Phys. **45**, 178–229, 1973

Vegard, L.: Hydrogen showers in the auroral region. Nature **144**, 1089–1090, 1939

Wax, R. L., Bernstein, W.: Rocket-borne measurements of Hβ emissions and energetic hydrogen fluxes during an auroral breakup. J. Geophys. Res. **75**, 783–787, 1970

Whalen, B. A., Miller, J. R., Mc Diarmid, I. B.: Evidence for a solar wind origin of auroral ions from low-energy ion measurements. J. Geophys. Res. **76**, 2406–2418, 1971

Whalen, B. A., Mc Diarmid, I. B.: Further low-energy auroral-ion composition measurements. J. Geophys. Res. **77**, 1306–1310, 1972

Received July 24, 1975